# Chapter 7
# Piezoelectricity and Ferroelectricity in Biomaterials: From Proteins to Self-assembled Peptide Nanotubes

V.S. Bystrov[1,2,*], I. Bdikin[1,3], A. Heredia[1], R.C. Pullar[1], E. Mishina[4], A.S. Sigov[4], and A.L. Kholkin[1]

[1] Department of Ceramics and Glass Engineering & CICECO, University of Aveiro, 3810-193, Aveiro, Portugal
[2] Institute of Mathematical Problems of Biology RAS, 142290, Pushchino, Russia
[3] Department of Mechanical Engineering, Centre for Mechanical Technology & Automation, University of Aveiro, 3810-193 Aveiro, Portugal
4 Moscow State Institute of Radioengineering, Electronics and Automation, 119454 Moscow, Russia
bystrov@ua.pt, vsbys@mail.ru

**Abstract.** Piezoelectricity is one of the common ferroelectric material properties, along with pyroelectricity, *etc*. There has been widespread observation of piezoelectric and ferroelectric phenomena in many biological systems and molecules, and these are referred to as *biopiezoelectricity* and *bioferroelectricity*. Investigations have been made of these properties in biological and organic macromolecular systems on the nanoscale, by techniques such as atomic force microscopy (AFM) and piezoresponse force microscopy (PFM). This chapter presents a short overview of the main issues of piezoelectricity and ferroelectricity, and their manifestation in organic and biological objects, materials and molecular systems. As a showcase of novel biopiezomaterials, the investigation of diphenylalanine (FF) peptide nanotubes (PNTs) is described in more detail. FF PNTs present a unique class of self-assembled functional biomaterials, owing to a wide range of useful properties, including nanostructural variability, mechanical rigidity and chemical stability. The discovery of strong piezoactivity and polarization in aromatic dipeptides [*ACS Nano* **4**, 610, 2010] opened up a new perspective for their use as nanoactuators, nanomotors and molecular machines as well possible biomedical applications.

## 7.1 Introduction

Piezoelectricity is one of the common ferroelectric material properties [1-3], along with pyroelectricity, optical birefringence phenomena, *etc*. Piezoelectricity in

* Corresponding author.

G. Ciofani & A. Menciassi (Eds.): Piezoelectric Nanomaterials for Biomedical Appl., EM, pp. 187–211.
springerlink.com 

organic and biological objects was first observed and described by Fukada in the 1950's [4] (initially in wood [4, 5], and later in bone tissue [6, 7]). Later, this phenomenon was also named *biopiezoelectricity.* Piezoelectricity arises from the electromechanical coupling in a given material [1-3]. This coupling is well known in biology - it can be observed in voltage-controlled muscle movement, the nervous system, ion transporters, etc. [8] - and it is at the heart of general ferroelectric and bioferroelectric phenomena.

Piezoelectricity and pyroelectricity have now been widely observed in various biological materials [8-21]. Lang *et al.* [16] were the first to report piezoelectricity in calcification of the human pineal gland, demonstrating this phenomenon by second harmonic generation (SHG) measurements, showing ferroelectric-related phenomenon in biological systems. Athenstaedt [22] noted that ferroelectricity may be common in biological cell components. Fröhlich [23] analyzed the effects of the high electrical fields found in biological membranes on the dipolar properties of the proteins dissolved them. It is significant that his model predicts the appearance of a ferroelectric or "quasi-ferroelectric" state. Following Athenstaedt's groundbreaking work, von Hippel predicted that "*... relations may exist between ferroelectricity, the formation of liquid crystals, and the generation of electric impulses in nerves and muscles*" [24]. Ferroelectricity is an example of the general phenomenon in which a system can be switched between two states of orientation by the application of a force [1-3, 8]. These phenomena are essential for many organic, biological molecules, and all living systems in our asymmetric universe. Such ferroelectric phenomena, essential for, and exhibited in, all living entities, now are named *bioferroelectricity* [8, 9].

Many current prospective nanomaterials for nanoelectronics, nanomedicine and biomedical applications, based on nanocrystals and liquid crystalline structures, as well on complex molecular, organic and biological structures, have a common feature: the dipole moment. This spontaneous dielectric dipole moment per unit volume is called the polarisation, and many such materials are called *ferroelectric*. This term shares a similarity with *ferromagnetic*, because the spontaneous polarisation can be reoriented by an external electric field, in the same way that magnetisation can be switched by magnetic field. This results in a hysteresis loop in the electrical polarisation, with a remanent polarisation at a zero applied field, and a reversible polarisation with an oppositely applied field in ferroelectrics. Both single phase and composite materials exist that have multiple *ferroic* switching properties (*e.g.* ferromagnetic and ferroelectric); these are called *multiferroic* materials [1-3, 8], but single phase multiferroics are rare.

One of the common peculiarities of ferroelectrics is the non-linear behaviour of the dielectric permittivity $\varepsilon$ under an external electric field $\boldsymbol{E}$, which distorts local charge distributions, in accordance with the Curie-Weiss law [1]. The Curie-Weiss law describes the relationship between magnetic or electric susceptibilities and

temperature, but it breaks down in the region very close to phase transition temperatures. This relationship is observed in the temperature behaviour of piezoelectric constants, as well as in the description of all ferroelectric materials [2], including ferroelectric liquid crystals [3], whose structures resemble certain biological systems such as biological excitable membranes composed from lipid bilayers and embedded protein structures (ion channels, receptors, *etc*.) [8]. Such ferroelectric materials (dependent upon symmetry class, see section 2 below) exhibit *piezoelectricity* (change of polarisation under an applied mechanical stress, and inversely a mechanical deformation under an applied electrical field), and *pyroelectricity* (temperature-dependent polarisation in certain anisotropic solids) [1-3, 8, 9]. Piezoelectricity is reversible under an external electric field, and the magnitude of the piezoelectric constant is dependent upon the spontaneous polarisation, as well as being sensitive to phase transitions, temperature, pressure and electrical and magnetic fields.

There are now many examples which show the wide range of the biopiezoelectric and bioferroelectric phenomena, observed in various biological and organic macromolecular systems at the nanoscale level [8-10]. These include novel nanobiomaterials, which are very important for various applications (in nanotechnology and biomedical fields), such as self-assembled diphenylalanine (FF) peptide nanotubes (PNTs) [10]. In the following sections, we will briefly discus and review the reported piezoelectric and ferroelectric properties of biological objects. We will then look at the main features of newly discovered strongly piezoelectric bionanomaterials based on FF PNTs, which could be highly appropriate for biomedical applications.

## 7.2 Biopiezoelectricity and Bioferroelectricity

### *7.2.1 Piezoelectric Phenomena in Biological and Related Objects*

Piezoelectricity is a phenomenon which can exist only in noncentrosymmetric materials [1-3]. The main building blocks of life are proteins, and the majority of protein crystals are noncentrosymmetric. Proteins are made of combinations of the 20 known amino acids, the majority of which also have noncentrosymmetric crystal structures. In the works of Lemanov *et al.* [25, 26] it was demonstrated that, as a consequence, these amino acids possess piezoelectric properties. He revealed the temperature-dependent piezoelectric response of amino acid crystals, and attributed it to enhanced damping of elastic vibrations in the crystals due to rotation of the $CH_3$ and $NH_3$ groups [25, 26].

Biopiezoelectricity is exhibited in large-scale biological systems such as proteins, biopolymers, polysaccharides, organelles and glands [4-26]. Some of the most

studied biological materials possessing piezoelectricity are bones, and especially one of bone's components - collagen fibrils, which contribute to bone elasticity. Collagen is an organic crystalline matrix of bone, composed of strongly aligned polar organic protein molecules [12]. Piezoelectricity in bones and tendons was discovered in 1957 by Fukada and Yasuda [6]. The shear piezoelectric coefficient of tendons was estimated to be $d_{14} = -2.0$ pC/N. Reports on the observation of the pyroelectric effect [13, 16-19] were the first evidence of the existence of macroscopic spontaneous electrical polarisation in bones. Application of an ac electrical field to cortical human bone made it possible to observe the reversal of the spontaneous polarisation, by recording a dielectric hysteresis loop [27]. Dozens of articles were subsequently devoted to this phenomenon in bones and collagen fibrils, showing a similar degree of piezoelectricity (0.8 pC/N) in different parts of the bone. Recently, the piezoelectric properties of bones [28] and collagen fibrils [29] have been studied with nanoscale resolution. It has been proposed that the piezoelectric effect plays an important physiological role in bone growth, remodelling and fracture healing. Recently a strong piezoelectric effect was observed and investigated in new bio-organic objects, such as bio-inspired self-assembled peptide nanotubes (PNTs) [10, 30].

As was already mentioned above, piezoelectricity arises from the *electromechanical coupling* in any given material [1-3]. We can assume that biopiezoelectricity similarly arises from electromechanical coupling in bio-organic molecular nanostructures.

The phenomenon is based upon the known general relation between the piezoelectric constant $d_{ik}$, the electrostriction coefficient $Q_{ik}$, the permittivity of the material $\varepsilon$, the permittivity of vacuum $\varepsilon_0$, and the component of polarisation $P_k$ of the whole system [1-3, 31]. For a simple case, as a first approximation for only one component of the coefficient $Q_{11}$, the piezoelectric constant $d_{33}$, dielectric permittivity ε and spontaneous polarisation $P$, the relationship can be written as [32]:

$$d_{33} = 2Q_{11}\varepsilon\varepsilon_0 P \tag{7.1}$$

On this basis, we can study piezoelectricity and related changes in the dipole moments and polarisation of various systems. For example, interesting direct observations piezoelectric contrast using piezoresponse force microscope (PFM) in biomaterials were made on bone samples by Halperin *et al.* [28] (see Fig. 7.1). They determined the values of dielectric constant $\varepsilon \sim 20$ and then the piezoelectric coefficients were evaluated for points 1-4 (Fig. 7.1a): 8.48 pC/N, 7.80 pC/N, 8.72 pC/N, and 7.66 pC/N, respectively.

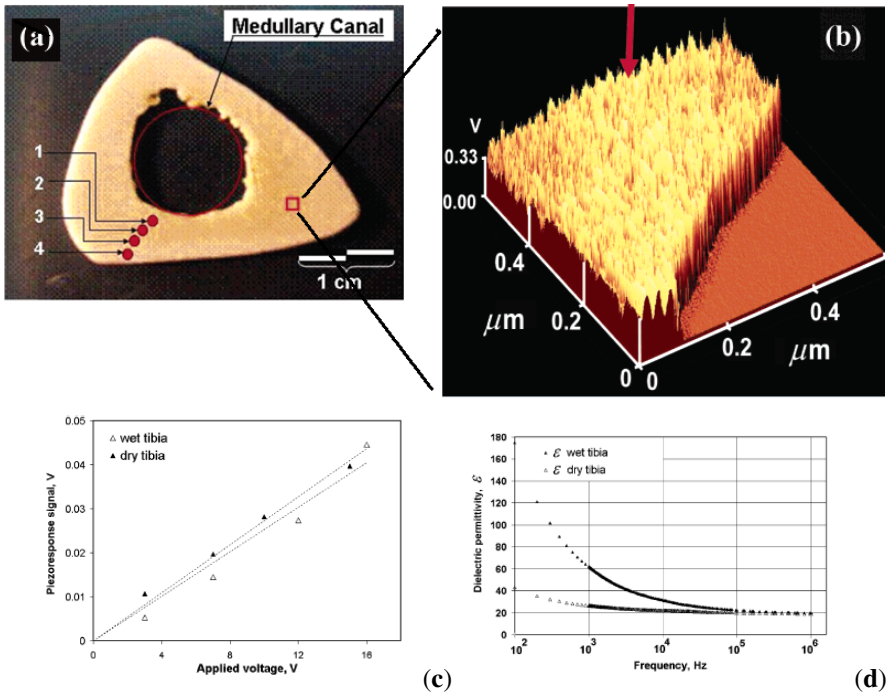


**Fig. 7.1** Experimental observations of piezoelectric effect and dielectric permittivity measurements on tibia bone samples (Reprinted with permission from [28]. Copyright 2004 American Chemical Society): (a) Transverse cut of tibia bone, piezoelectric coefficient was measured in four marked points. (b) Piezoresponse image with nanoscale resolution (marked as a square region on (a)). (c) Piezoelectric response measured in wet and dry tibia. (d) Dielectric response measured in wet and dry tibia.

### *7.2.2 Ferroelectric Phenomena in Biological and Related Systems*

The ferroelectric properties of several biological objects, materials and molecular systems have been investigated [8-10, 32], one of the most notable being *biological membranes.* Interesting studies were made by Beresnev *et al.* [33] noting the close similarity between biological membranes and ferroelectric liquid crystals, particularly the presence of a layered structure with tilted lipid and protein molecules (*e.g.,* chiral molecules of cholesterol). They proposed ferroelectricity as the physical mechanism responsible for the propagation of excitation in such biomembranes [33]. The proposal that the lipid bilayer of biomembranes acts as a voltage sensor in excitable membranes was made by Pikin *et al.* [34]. Later Leuchtag directly showed that this role was played by a special self-organized ferroelectric-like mechanism in the voltage-sensitive ion channels of the excitable biomembranes [8, 43]. Several ferroelectric-related

phenomena have also been observed by Tasaki in biomaterials and biological membranes. For example, linear electro-optic effects connected with polarisation changes have been found in nerve fibres in a series of piezoelectric, light scattering and birefringence measurements, under the excitation process of nerve impulse propagation along axons [35, 36]. It was established that excitable membranes and ion channels exhibit properties characteristic of ferroelectrics, including critical temperatures, hysteresis, pyroelectricity and surface charges [8, 9]. On this basis, Leuchtag proposed a functional role for ferroelectric phase transitions in ion channels [8, 9, 43]. These days biological membranes are described as complex composite ferroelectric systems [8], which consist of lipid bilayers embedded with various proteins and other biomacromolecules and molecular structures.

*Ion channels* are the macromolecular components of the membranes of nerve and muscle cells responsible for impulse conduction. Embedded into the phospholipid bilayer bounding the cell, these large glycoprotein molecules act as voltage-dependent switches. In response to changes in the voltage across the membrane, they undergo conformational transitions between two states ("close" and "open"), in which they become permeable to specific sets of ions (*e.g.,* $Na^+$ or $K^+$) [8, 30]. This is very similar to the switching phenomena in ferroelectrics [1-3, 9]. The ferroelectric channel unit model, proposed by Leuchtag [8, 9, 43], was later developed into the ferroelectric liquid crystal model [9, 37] for ion channels of excitable biomembranes. The possibility of the involvement of ferroelectric phenomena in biological membrane function was also suggested by several other authors: Tokimoto *et al.* analyzed a ferroelectric model of nerve conduction as a stable limit cycle and self-organized model [38, 39], Bystrov *et al.* applied the Landau–Ginzburg equation to nonlinear waves in biomembranes with ferroelastic as well as ferroelectric phases [40], and analysis by Gordon *et al.* of a ferroelectric liquid crystal model described the action potential as a travelling kink-like excitation [41].

The most systematic study of bioferroelectric phenomena was made by Leuchtag [8, 9, 43]. His direct observation of ferroelectric phenomena in biological membranes and ion channels was made by the fitting the capacitance measurements. This clearly showed that the temperature dependence of the capacitance of squid axon membranes recorded by Palti and Adelman [42] obeys the *Curie–Weiss law* [43] for ferroelectrics (see Fig. 7.2).

$$\varepsilon = C_W / (T_0 - T), \quad T < T_C \tag{7.2}$$

where $C_W$ is the Curie-Weiss constant, $T_0$ is the Curie point and $T_C$ is the phase transition point.

For membrane capacitance $C$ (per unit area) containing ion channels as parallel array

$$C = C_0 + k / (T_0 - T), \tag{7.3}$$

where

$$k = \varepsilon_0 a\, C_W / L, \tag{7.4}$$

and $a$ is defined as the area fraction occupied by the ion channels, $L$ the membrane thickness and $\varepsilon_0 \sim 8.854$ pF/m is a permittivity of vacuum. From fitting data there were determined values of $T_0 \sim 49.80$ °C and $C_W \sim 800$ K below $T_C$ and ~ 6400 K above $T_C$ [43]. This data indicates that the ion channel transition falls within Group II of order-disorder transitions [1 -3, 8]. The phase transitions in this group are explained by a model of reversible or rotatable permanent dipoles, which in a parallel orientation give rise to spontaneous polarisation below the Curie point, but which lose that polarisation when the order is lost above the Curie point. A crystalline ferroelectric, sodium nitrite, $NaNO_2$, has a comparable Curie constant of 5130 K, with a Curie point of 164°C [43].

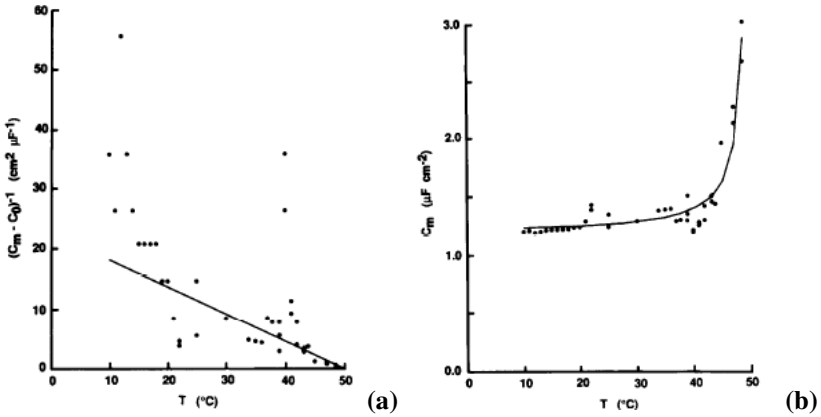


**Fig. 7.2** Dielectric anomaly of squid axon membrane fitted to the ferroelectric Curie-Weiss law (Reprinted with permission from [43]. Elsevier Copyright 1995 Clearance Center): (a) Least-squares linear regression fit of reverse capacitance versus temperature, derived from the ferroelectric Curie-Weiss law (the points are from membrane capacitance versus temperature data of Palti and Adelman [42], presented in [43]); (b) Membrane capacitance versus temperature (the points are from Palti and Adelman [42]).

Liquid-crystal-like ferroelectric transitions controlled by temperature and electric field were observed in the purple membrane of the bacterium *Halobacterium salinarium* [44] (see Fig. 7.3). A dielectric spectroscopy study of oriented purple membranes has shown that *bacteriorhodopsin*, which is an integral membrane protein, possesses a significant electrical dipole moment and demonstrates a liquid-crystal-like ferroelectric behaviour [3, 44].

These experiments were the direct confirmation of the theoretical model of ferroelectric-like behaviour of ion channels in excitable biological membranes [8, 9, 37], which acted as electric switches between ferroelectric (closed, insulating) and paraelectric (open, ion-conducting) states.

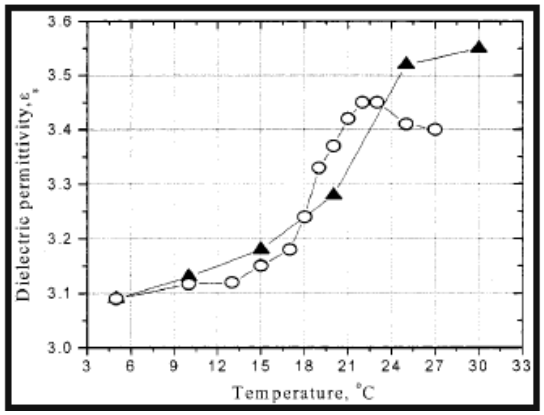


(a)

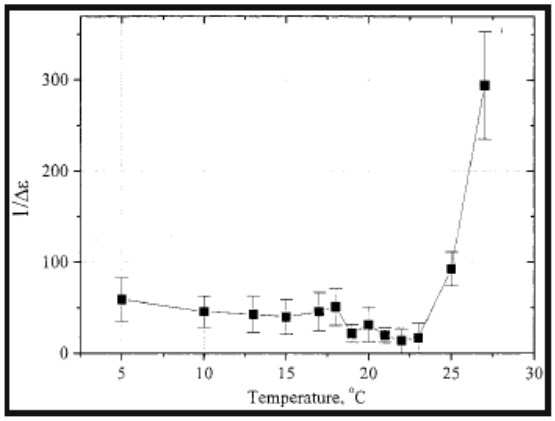


(b)

**Fig. 7.3** Observation of liquid-crystal-like ferroelectric behaviour in a biological membrane (Reprinted with permission from [44]. Copyright 2001 American Chemical Society): (a) Temperature dependence of the dielectric permittivity of the Bacteriorhodopsin (bR) membrane in the low-frequency limit of time domain dielectric spectroscopy (TDDS) measurements; (**Δ**) denotes heating of sample; (O) denotes cooling of sample. The measurement accuracy of the dielectric permittivity was better than 3%. (b) Temperature dependence of the inverse dielectric strength.

It must be emphasized that these phenomena connected with the Curie-Weiss law are observed in all piezoelectric response experiments as well, *e.g.,* in the temperature dependence of piezoelectric modulus in the vicinity of phase transition points [1-3, 8], as well its changes under electric field alteration [1-3, 8]. They are also observed at the nano-scale level in measurements of various piezoelectric switching processes, including the local hysteresis loop, which is now widely measured by the PFM technique in different organic and biomolecular structures [10, 30], and this is discussed in more detail in section 7.3.

Another important example of piezoelectric and ferroelectric properties and behaviour in the interior of biological objects is to be found in the interior structure of cells, in *microtubules* [45]. Microtubules of nerve cells are a stable relative to their counterparts in the rest of the body, this stability allowing them to participate in cellular signalling and transport processes**.** Each microtubule is a cylindrical protein structure, and they are the major constituent part of the cytoskeleton of all eukaryotic cells. They are hollow tubes, whose walls are assembled from molecules of the globular protein *tubulin* [45], and have an electric dipole moment that contributes to the overall polarity of the structure. Microtubule dipolar lattices have been reported to exhibit piezoelectric properties [12, 45] (assuming the Young's modulus of microtubules, E=1.4 GPa [46]), and have a ferroelectric phase [47].

In recent articles [48, 49] by Tuszynski *et al.*, the dielectric properties of several biomolecules and biomolecular assemblies were discussed, especially polymer ferroelectrics such as polyvinylidene fluoride (PVDF), as well as tubulin, microtubules and voltage-gated ion channels. The emphasis in this paper was placed on identifying the potential for the occurrence of bioferroelectricity, and its role in biological functions, in particular self-assembly and control of mass and charge transport. There is an urgent need now for experimental and theoretical estimates of the value of the dielectric constant of tubulin, as a crucial quantity defining the ferroelectric properties of microtubules, especially at the level of individual nano-scale components forming biological structures. In addition, the last is very important for biomedical applications, such as, *e.g.*, the searching of new medical anti-cancer drugs.

### *7.2.3 Piezoresponse Force Microscopy (PFM) for the Study of Bioferroelectrics on the Nanoscale*

The most appropriate and useful methods of such nanoscale studies are atomic force microscopy and piezoresponse force microscopy (AFM and PFM) [21, 50-52]. Using these AFM techniques, the mechanical properties of single microtubules were tested by lateral indentation with the tip of the AFM [53, 54]. The estimated value of Young's modulus was between 0.04 and 1.2 GPa from these bending experiments, but measurement with PFM has not yet have been carried out. The biological importance of the piezoelectric effect in microtubules remains to be assessed, but it should be noted that recent studies on microtubules show *the similar nature of microtubules and peptide nanotubes, both connected with amyloid fibrils* [55].

Understanding the relationship between physiologically generated electrical fields and mechanical properties on the molecular, cellular and tissue levels has become the main motivation for studying piezoelectricity in biological systems at the nanometer scale. A very strong electromechanical response has been found in human enamel and dentin, attributed to protein fibrils (presumably collagen) embedded within a non-piezoelectric matrix. PFM made it possible to image the

spiral shape and orientation of protein fibrils with a 5 nm spatial resolution. The orientation of chitin molecular bundles in a butterfly's wing has also been demonstrated by this technique [56, 57].

For bioapplications in devices such as transducers and biosensors, or as components of biomedical drug/delivery systems, nanomaterials must be compatible with the surfaces of the biological objects involved, particularly physical, mechanical and electrical parameters. Several such nanomaterials (the polymer ferroelectric PVDF and its composites with lipids, amino acids, diphenylalanine (FF) peptide nanotubes (PNTs)) have been studied by various nanoscale methods. AFM, PFM, electrochemical strain microscopy (ESM), XRD, etc., have been used to characterise local piezoresponse properties, nanoscale structure and switching behaviour, corroborated with computational molecular modelling [50]. These studies directly showed that ferroelectricity can exist at the molecular and nanoscale, and consequently is an essential property small biological objects, such as molecular components of cells, and membranes such as ion channels, microtubules, *etc*. We must further study these ferroelectric switching phenomena in living molecular systems, and then exploit their nature effectively for technical and biomedical applications.

In the following section we describe the results of our studies of FF PNTs, focused on its possible biomedical applications.

## 7.3 Piezoelectric and Ferroelectric Properties of Self-assembled Diphenylalanine Peptide Nanotubes (FF PNT)

Self-assembled diphenylalanine (FF) peptide nanotubes (PNTs) represent a novel and unique class of self-assembled functional biomaterials, owing to the wide range of their useful properties, including nanostructural variability, mechanical rigidity and chemical stability. FF PNTs are promising objects for a vast array of nanotechnology applications including biosensors, nanotemplates, ultracapacitors, *etc*. The discovery of strong piezoelectric activity, temperature-dependent spontaneous polarisation and phase transition [30] in these aromatic dipeptides established them as nanomaterials with ferroelectric properties. This opened up a new perspective for their use as nanoactuators, nanomotors and molecular machines, as well as wide ranging novel applications for which a piezo- and ferroelectric material would be essential [58]. Piezo-, pyro- and ferroelectric properties of materials, especially self-assembled nanomaterials, have been at the heart of many technological advances over the years in fields as far ranging as electronics [59], sensors [60], biomedical imaging [62, 63] and data storage [64].

### *7.3.1 Organic Biomolecular Ferroelectric Materials and Dipeptide Nanotubes*

Organic ferroelectrics offer a potential cost advantage and flexible deposition and control, as well as self-assembly features (especially self-assembling organic nanotubes based on the linear and cyclic peptide architecture), all of which are not available in inorganic ferroelectrics [64-75]. Many proteins and polysaccharides

are actually piezoelectric due to the presence of polar bonds, and some biomolecules with bias-induced conformational states can be thought of as being ferroelectric. They are inexpensive, and their structure can be easily modified through chemistry, which makes them highly versatile. Peptide-based systems are of particular importance from the biological of view, as models for ion channels, membranes, amyloid fibrils, *etc*. [76-79]. For this group of materials, tube-like structures are easily formed by stacking aromatic rings through the formation of hydrogen bonds between functional groups in the backbone structure, and related to aromatic $\pi$–$\pi$ interactions [80]. A common self-assembly process for small aromatic dipeptides involves the assembly of diphenylalanine (FF), $NH_2$-Phe-Phe-COOH, monomers into peptide nanotubes (PNTs), and this was studied in detail by Gorbitz [81-83] and the group of Gazit [78-80, 84, 85].

These PNTs had first been discovered from the determination of the smallest recognition motif of the amyloid-$\beta$ protein, associated with over 30 diseases, mostly neurodegenerative ones such as Alzheimer's, Huntington's, Parkinson's, Creutzfeldt–Jacob and prions, but also sclerosis (Lou Gehrig's disease) and type-II diabetes [86]. They are made from amino acids, self-assembled in uniquely stable tubes with hydrophilic hollows [67], having a high Young's modulus and chemical stability [85].

X-ray and electron diffraction studies have revealed that their room temperature crystal structure is compatible with the space group $P6_1$ [81], allowing many physical phenomena described by the odd-rank tensor, including optical second harmonic generation, pyroelectricity, linear electro-optic effect and piezoelectricity. Crucial for applications is the temperature dependence of polarisation in FF PNTs, and the possible phase transformation under heating above room temperature. It was shown [31] that FF PNTs are also strongly piezoelectric, with the orientation of polarisation along the tube axis, and demonstrated a temperature-dependent polarisation response [32], studied via PFM [21, 51, 52] and the optical Second Harmonic Generation (SHG) method. These measurements show a gradual decrease in polarisation with increasing temperature, accompanied by an irreversible phase transition into another crystalline phase at about 140–150ºC. The results are corroborated by the molecular dynamic simulations, predicting an order–disorder phase transition into a centrosymmetric (possibly, orthorhombic) phase with antiparallel polarisation orientation in neighbouring FF rings. Partial piezoresponse hysteresis indicates incomplete polarisation switching due to the high coercive field along the tube axis in the virgin FF PNTs. However, the attempts to switch polarisation in this material were unsuccessful due to geometry and high coercive voltage observed in the nanoscale ferroelectric measurements, and also through molecular simulations [30]. Below we present some results of these studies in more detail.

### *7.3.2 Diphenylalanine Peptide Nanotubes. Preparation and Investigation*

Self assembled FF PNTs were prepared as previously reported [69], their composition and physical structure were confirmed by x-ray diffraction (XRD)

and scanning electron microscopy (SEM), and their nanostructure and piezoelectric properties were investigated by AFM/PFM techniques, as shown in Fig. 7.4 [30, 50-52] for In-plane (IP) and Out-of-plane (OOP) piezoresponse measurements. The computational molecular modelling of the FF PNTs' physical and electronic structure, their electrical properties and dynamic behavior under electrical field and temperature alterations, were performed by molecular modeling and molecular dynamic (MD) simulations, using HypeChem versions 7.52 and 8.0 [50, 87]. The short overview of the results is given in this section.

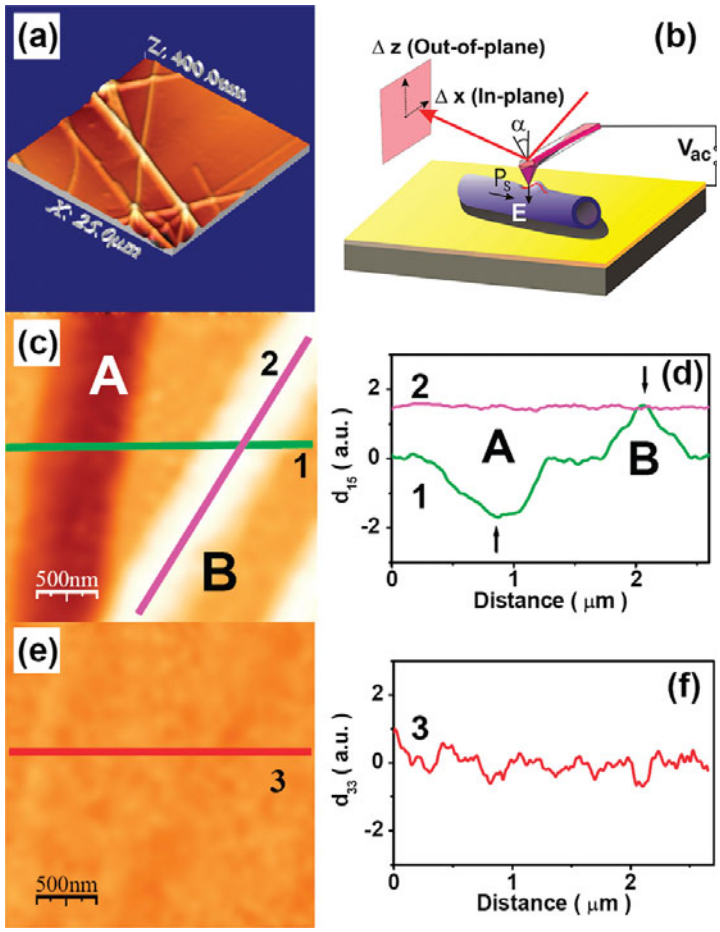


**Fig. 7.4** Schematic of AFM/PFM experimental tools and some results (Reprinted with permission from [30]. Copyright 2010 American Chemical Society): (a) Topography of as-deposited PNTs on Au-coated substrate (scan 25 x 25 $\mu m^2$), (b) schematic of the nanoscale in-plane (IP) measurements by PFM, (c) IP piezoresponse of two tubes (A and B) with oppositely directed polarisations, (d) cross sections of the IP image across (1) and along (2) the tube axis, demonstrating different sign and uniformity of polarisation, (e) OOP image of the same tubes, and (d) cross section of (e) along line 1 $V_{ac} = 2.5$ V, $f = 5$ kHz.

Figure 7.5 shows the representative SEM and PFM images of the fabricated PNT, assembled horizontally and vertically on metallized substrates as described above. A variety of tubes of different lengths, diameters and orientations were obtained. A strong piezoelectric contrast was seen on both horizontal (*via* lateral PFM signal, inset to figure 7.5(a)) and vertical tube assemblies (*via* vertical PFM, inset to figure 7.5(b)). These results confirm the already published data [30] on horizontal tubes, where only the shear piezoelectric coefficient ($d_{15}$≈60 pmV$^{-1}$ on sufficiently big tubes) could be measured. The estimate of the effective longitudinal piezoelectric coefficient $d_{33}$ in vertical tubes yields values in excess of 30 pmV$^{-1}$, *i.e.* it exceeded that for $LiNbO_3$ [88].

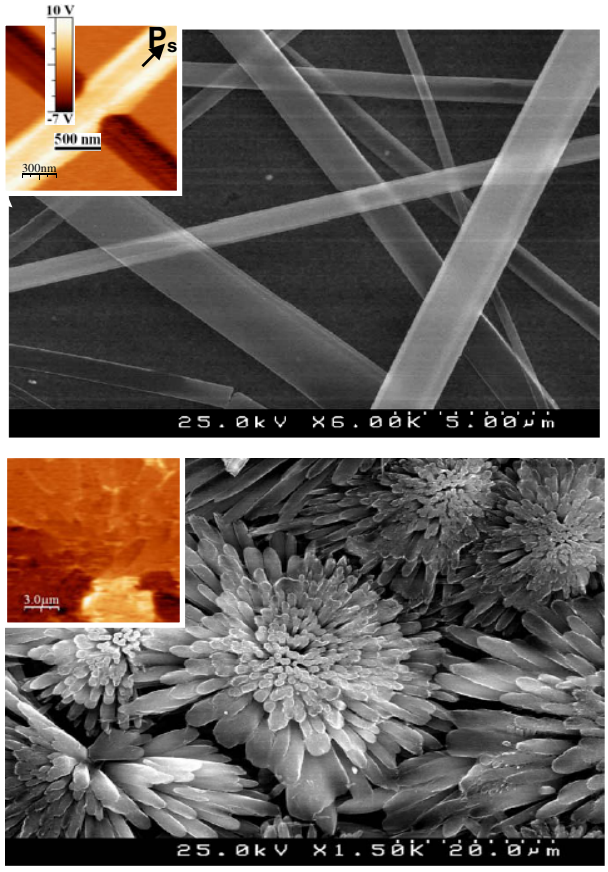


**Fig. 7.5** Representative SEM images of horizontal (a) and vertical (b) peptide nanotube array. Insets show corresponding PFM images. (Reproduced from [50] with permission by IOP Publishers.)

Figure 7.6*(b)* represents the variation of the average shear PFM contrast with increasing temperature measured on horizontal tubes. The contrast gradually decreases with temperature, demonstrating monotonic $d_{15}$ dependence and ultimate disappearance of piezoresponse at a temperature of ~150 ºC. It should be noted that the contrast becomes irreversible if the sample is heated above 100 ºC, *i.e.* it is not recovered after cooling down to room temperature and remains practically zero after heating up to 140–150 ºC. This hints at the possible phase transformation to another phase on heating, as no visible degradation of the topography was found.

Figure 7.6(a) shows the temperature dependence of second harmonic generation (SHG) intensity measured on vertical tubes (both heating and cooling runs), which are compared with the molecular dynamics (MD) calculations [50]. The results are, in general, consistent with the temperature-dependent PFM contrast measurements. Eventually, the SHG signal decreases at ~130 ºC (irreversibly as shown by the cooling curve). It should be noted that these data are consistent with recent studies of thermal stability of PNTs [89].

These measurements revealed that FF PNTs exhibit a phase transition between two piezoelectric phases, as confirmed by the existence of piezoresponse both below and above the transition in the temperature range 100-150 $^{o}$C. Details of this phase transition are now being investigated and will be reported in the future. In general, the apparent decrease in the piezoelectric contrast and SHG intensity (Figure 7.6) with temperature is a clear signature of an irreversible phase transformation to a high-symmetry phase, as is often observed in molecular crystals [90, 91]. The XRD patterns of the vertical PNTs were measured before and after temperature annealing at 150 ºC for 1 hour. In virgin samples (grown at room temperature), all observed peaks correspond to the expected hexagonal structure already reported for FF PNTs (a=24.071 Å, c=5.456 Å, α=120°, space group $P6_1$) [81]. The diffraction peaks for annealed PNTs are apparently different, belonging to another crystalline phase. All diffraction peaks after annealing could be explained based on the appearance of an orthorhombic structure with the unit cell parameters: a=5.210 Å, b=24.147 Å, c=41.072 Å.

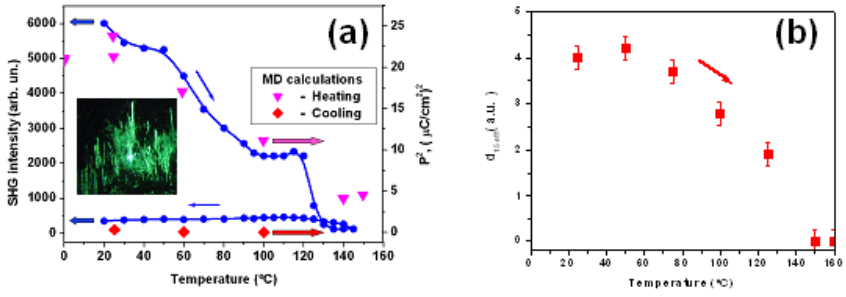


**Fig. 7.6** Temperature dependencies of SHG (a) and PFM signals (b) for FF PNTs. The data points on SHG curves are compared with the MD calculations undertaken for parallel double-stacked FF in the hexagonal phase (triangles) and anti-parallel ones in the orthorhombic phase (diamonds). (Reproduced from [50] with permission by IOP Publishers.)

The possible phase transition between hexagonal and orthorhombic phases upon annealing is illustrated in Figs. 7.7b and 7.7c, which show how the initial hexagonal unit cell could be transformed into the orthorhombic one *via* a small deformation of the FF rings. The mainframe of the FF PNT structure consists of the FF rings (Fig. 7.7a), formed from six individual FF molecules (6FF), in accordance with Görbitz [81]. Each ring possesses a dipole moment $P_s$ along the tubular OZ axis perpendicular to the ring plane, and forms the hexagonal structure [81] from four rings (Fig. 7.7a, right). It is suggested that for the hexagonal structure all 6FF rings (A, B, C, and D) have the same orientation as the individual $P_s$ (Fig. 7.7b), this being compatible with the total large dipole moment and strong piezoresponse in PNTs grown at room temperature [31, 32]. Antiparallel orientation of $P_s$ for the neighbouring 6FF rings (A and C opposite to B and D) produces novel orthorhombic structure with zero total polarisation (Fig. 7.7c) for annealed tubes.

To understand further the molecular structure of the FF PNTs, and the possible mechanisms of their self-assembly and phase transitions, the molecular modelling and molecular dynamic (MD) simulations were we performed using HypeChem 7.52 and 8.0 [87]. The isolated ring with six dipeptides, as well the parallel stacking of two rings (see Fig. 7.8), were studied by the geometry optimisation of the total energy, and MD runs using molecular mechanics (MM) methods (BIO CHARM) in combination with a first principle quantum approach (*ab initio* and PM3 semi-empirical, in UHF approximation).

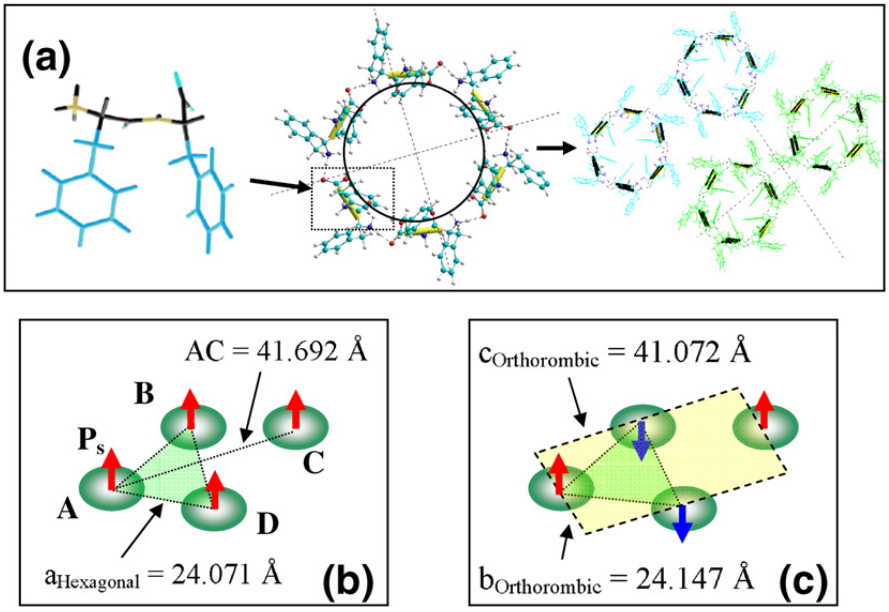


**Fig. 7.7** (a) Schematic illustration of the self-assembly process of PNTs: from individual diphenylalanine (FF) monomer molecules to six dipeptides (6FF) forming a ring and finally to whole structure of peptide nanotubes. Models of the hexagonal (b) and orthorhombic (c) structures of PNTs (detailed explanation is given in the text). Reproduced from [50] with permission by IOP Publishers.

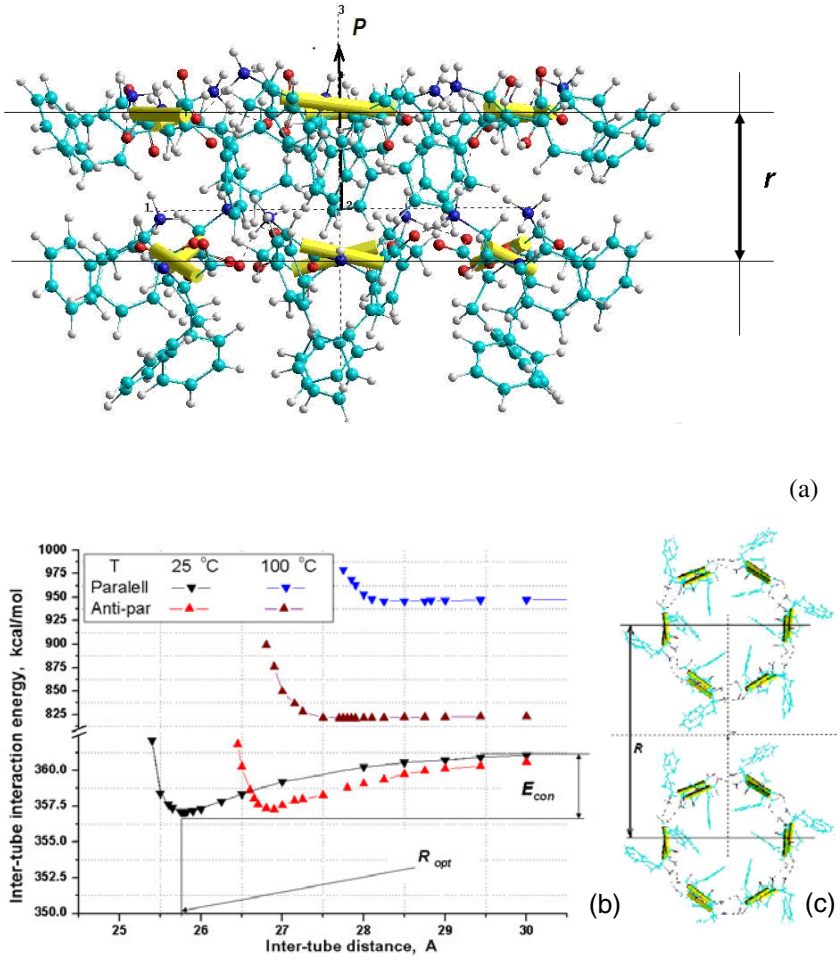


**Fig. 7.8** Molecular model of the FF ring and double-ring formation leading to the large cooperative dipole moment in PNT structure (a), depending on the inter-ring ($r$) and inter-tube ($R$) distances schematically shown in (a) and (c). Calculated variation of inter-tube condensation energy $E_{con}$ with distance $R$ (b) and comparison of minimum energy distances for two different temperatures for parallel (hexagonal) and anti-parallel (orthorhombic) structures of PNTs (inset). Here the yellow tube denotes schematic presentation for tubular coil of main molecular unit $NH_2$-…-COOH. Reproduced from [50] with permission by IOP Publishers.

It was found that 6FF forms ordered rings (hexagonal structure, $P6_1$) with inner and outer diameters of ~10.5 and 25 Å, respectively (Fig. 7.7a, middle picture), connected by N-H...O hydrogen bonds with O-H lengths of ~1.65 Å and total N-O lengths of ~ 2.7 Å. This is in full agreement with the results of Görbitz [81].

Furthermore, we calculated the dipole moment as being ~1.3 Debye for a single 6FF ring, directed along the OZ hexagonal axis, corresponding to a spontaneous polarisation of $P \approx 0.24$ μC/cm$^2$. This data also corresponds to the reported values for isolated FF units [81, 32] (Fig. 7.7a). Figure 7.8 represents the next model of parallel double-stacked 6FF units. The optimisation for this model leads to an increase of dipole moment from ~ 1.3 Debye up to $D_t$ ~ 42 Debye (polarisation $P \sim 4.0$ μC/cm$^2$) and furthermore up to value $D_t$ ~ 52 Debye and polarisation value reaches $P_s$ ~ 5 μC/cm$^2$ [50]. These two FF rings (Fig. 7.8a) were connected by N-H...O hydrogen bonds with O-H lengths of ~1.88 Å and total N-O lengths of ~ 2.9 Å.

On the basis of this model, we performed MD runs and simulations at different temperatures. The result is fully consistent with the experimentally obtained SHG and PFM data, *i.e.*, the average dipole moment gradually decreases as a function of temperature (*cf.* calculations with experimental data in Fig. 7.6a). The polarisation is about 5 μC/cm$^2$ at 25 ºC and decreases to the value ~2 μC/cm$^2$ at 100 ºC. The results for a parallel stacked FF ring model correspond to the hexagonal phase and the experimentally observed large dipole moment and high piezoelectric coefficient in virgin structures, while the antiparallel orientation of neighbouring tubes correspond to the orthorhombic phase with a very small total dipole moment, as is shown in Fig. 7.6a. Moreover, this result made us believe that the dipole ordering along OZ hexagonal axis for the hexagonal phase is due to a cooperative dipole effect (as common to ferroelectric systems, while the orthorhombic phase is similar to antiferroelectrics), and polarisation switching is possible if a high-enough electric field is applied along this axis [30, 50].

### *7.3.3 Electric Field and Temperature Influence: Discussion on Phase Transition Nature*

Following the findings above, the measurement of the piezoresponse hysteresis on virgin (not annealed) vertical PNTs was performed [50]. The preliminary simulation data has led to the conclusion that the corresponding coercive field would be very high, in the order of ~30 MV/cm, and have an asymmetric character as a result of the strong internal bias field. This prediction is fully consistent with the experimental result (Fig. 7.9), where a hysteretic-like dependence of the effective $d_{33}$ *versus* applied bias is obvious. However, the loop reveals partial switching of the polarisation along the hexagonal axis with superimposed linear behaviour that could be caused by the electrostatic contribution to the piezoresponse (Maxwell stress) [31, 32]. Taking into account some flexibility of the PNTs at the contact point, and apparent non-local electrostatic interaction, this possibility cannot be ruled out. The results are in line with recent piezoresponse measurements on PZT nanotubes, where a similar character of the piezoresponse hysteresis was found [92]. This signifies that the local measurements in such complex geometries can be overshadowed by the spurious signals, irrespective of the nature of the material. The polarisation offset observed in the hysteresis loops (see Fig. 7.9) could be due to the fact that the available electric field is insufficient for switching, and only a small reverse

domain (unstable with time) is formed under a maximum bias. This is confirmed by the absence of any switched polarisation after the consequent PFM imaging. Since the available electric field from the tip is quite low (in the first approximation ~100-200 kV/cm under a bias of 10 V), this reduces the opportunities for using vertical FF PNTs as media for high density data storage. Unfortunately, higher biases destroy the tubes. Molecular simulations made under an electrical field were in line with the experimental observation, and showed that the antiparallel field of about 5 MV/cm is only able to decrease the polarisation value by about 12% [50]. But question still open for another opportunity of polarisation switching in perpendicular to PNT axis direction, especially for annealed PNT.

This question is our future work and the results to be published elsewhere soon.

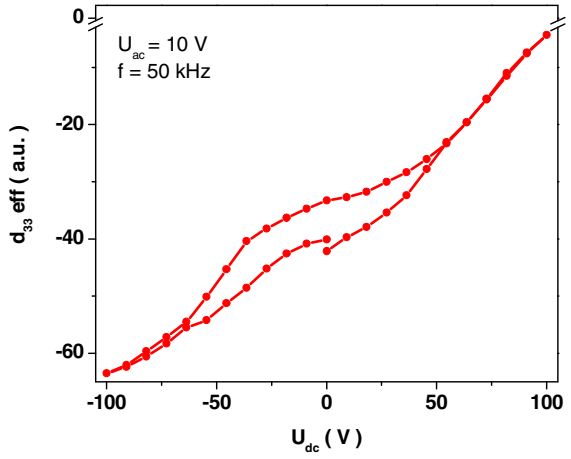


**Fig. 7.9** Out-of-plane piezoresponse hysteresis taken on vertical PNTs. The piezoresponse signal does not change sign even at a maximum bias, due to the high coercive field of the hexagonal structure. Reproduced from [50] with permission by IOP Publishers.

Another important result of our simulations is the tentative explanation of the observed hexagonal-orthorhombic irreversible transformation, because the calculations show that the temperature increase leads to the strong changes in the condensation energies, in particularly modifying inter-tube interaction. The approach for the inter-tube interaction calculations with distances, and determination of the condensation energies, is similar to that used by Nakanishi *et al.* [93]. As a result, the inter-tube condensation energy is decreasing with temperature rise and, at a temperature of about 150 $^{o}$C, it becomes comparable with the thermal energy kT (Fig. 7.8b). This ultimately leads to the dissociation of the PNT tubes and reorganisation of their structure, so that the antiparallel orientation of the rings becomes energetically favourable at high enough temperatures. All in all, the predicted re-orientation of polar molecular dipole

groups in neighbouring FF tubes leads to the compensation of the total polarisation to almost zero value, accompanied with the symmetry change and increase of the unit cell size. These results clearly show that for FF PNTs prepared at room temperature, the parallel orientation of the polar moments related to individual nanotubes is energetically favourable; while at $T \geq 150\ ^{o}C$ the preferred conformation is anti-parallel leading to a doubling of the unit cell. This model is in line with the experimental XRD results, and the orthorhombic structure shown in Fig. 7.7c. Upon cooling, this phase persists down to room temperature, being metastable within an extended period of time. The calculated transition temperature (see also on Fig. 7.6) is close to that observed by PFM and SHG experiments [50]. AFM and SEM data [50] indicate a notable degradation of the tube surface consistent with earlier reports [84].

It is already well known that FF peptides could form various supra-molecular structures. One of the most studied conformations is a hexagonal molecular nanotube structure, similar to that observed in liquid crystals (LC) [77, 94]. From this point of view it is evident that the studied PNTs could be considered as an analogue of a smectic C* (SmC*) phase, composed of six FF L-chiral molecules arranged as a single 6FF stable ring (one smectic disc further forms discotic-like columnar structure [90, 95]). Obviously, such a molecular LC is prone to polymorphic transformations [91] that occur due to a very wide variation of the peptide´s bond torsion angle [50, 81]. Some of these polymorphic phases could be metastable, leading to possible irreversible phase transitions. It is worth noting that structural polymorphism exists in the amyloid fibrils related to PNTs [96]. Similar transitions were observed in the temperature dependence of LC lipid systems [97], and in DNAs that change from tubular hexagonal to orthorhombic structure [98]. It is clear that our results resemble the well-known phase transition in LC from ferroelectric-like SmC* to paraelectric SmA phase. The details of the molecular simulations and calculations of the condensation energies are reserved for future publication.

## 7.4 Conclusions

In conclusion, our measurements revealed an important feature of the polarisation behaviour in self-assembled diphenylalanine peptide nanotubes (FF PNTs). As confirmed by the PFM and SHG measurements, the polarisation gradually decreases from room temperature to 140 ºC, and experiences irreversible phase transformation to another (probably orthorhombic) crystalline phase with zero polarisation. This phase persists upon cooling to room temperature. Partial polarisation switching is observed by the application of a strong electric bias to the PFM tip, but full switching is impossible due to the high coercive field. This result is in line with the fact that ferroelectric-like behaviour is originated from hydrogen bonds among the FF monomers, which break upon the temperature increase. This transformation is extremely important in view of the foreseeable applications of PNTs as sensors and actuators.

The new data obtained on piezoelectric and ferroelectric properties in the diphenylalanine peptide nanotubes are well correlated with several reports on the ferroelectric and piezoelectric properties in other organic and biological macromolecular structures (such as ion channels [8, 9, 30, 39-41], amino acids [25, 26], microtubules and tubulin [45-50, 53, 54], collagen [28], chitin [56], proteins and so on [10, 21, 52, 57]), and surely complement our understanding of these *biopiezoelectric* and *bioferroelectric* phenomena in living systems. Once we understand the role of ferroelectricity and piezoelectricity in nature, it would lead us not only to the progress in scientific knowledge, but also to the ability of designing new systems which copy nature or are inspired by it [8-10]. The results reported here are only our initial experiments with directly measured piezoresponse data, and first approximation for idealized molecular models. These initial simulations were performed on a reduced model, with some parts of the PNT removed (a 2-ring model of tube), owing to restriction of computer memory resources, *etc*. Probably, as a matter of fact, this annealing phase with oppositely-oriented and mutually compensated dipoles could be considered as an antiferroelectric phase, similar to some examples of biologically ordered molecular structures, such as in lipids [99]. Another interesting problem is measuring the actual switching properties of the piezoresponse and polarisation at the nanoscale level, and observation of the full hysteresis loop. All these questions require further investigation.

**Acknowledgements.** The work is supported by the Ministry of Science and Education of Russian Federation (Federal Special-Purpose Programme 'Cadres', contract No 02.740.11.560). VB is thankful to FCT (Portugal) for the partial financial support through his grant SFRH/BPD/22230/2005. IB and RCP would like to thank the Program Ciência 2008 of the Portuguese Science and Technology Foundation (FCT). We also acknowledge FCT projects PTDC/CTM/73030/2006 and REDE/1509/RME/2005 for partial support.

## References

[1] Lines, M.E., Glass, A.M.: Principles and Applications of Ferroelectrics and Related Materials. Clarendon Press, Oxford (1977)
[2] Smolenskii, G.A., et al. (eds.): Physics of Ferroelectric Phenomena: Ferroelectrics and related materials (1985) (Nauka, Leningrad, in Russian; Gordon and Breach, New York, in English)
[3] Goodby, J.W., Blinc, R., Clark, N.A., Lagerwall, S.T., Osipov, M.A., Pikin, S.A., Sakurai, T., Yoshino, K., Zeks, B.: Ferroelectric liquid crystals: Principles, properties and applications. Gordon and Breach, Philadelphia (1991)
[4] Fukada, E.: Vibrational study of the wood used for the sound boards of pianos. Nature 166, 772–773 (1950)
[5] Fukada, E.: Piezoelectricity of wood. J. Phys. Soc. Jpn. 10, 149–154 (1955)
[6] Fukada, E., Yasuda, I.: On the piezoelectric effect of bone. J. Phys. Soc. Jpn. 12, 1158–1162 (1957)
[7] Fukada, E., Yasuda, I.: Piezoelectric effects in collagen. Jpn. J. Appl. Phys. 3, 117–121 (1964)

[8] Leuchtag, H.R.: Voltage-Sensitive Ion Channels: Biophysics of Molecular Excitability. Springer, Dordrecht (2008)
[9] Leuchtag, H. R., Bystrov, V. S., Theoretical models of conformational transitions and ion conduction in voltage-dependent ion channels: Bioferroelectricity and superionic conduction. Ferroelectrics 220 (3-4), 157-204(1999)
[10] Amdursky, N., Beker, P., Schklovsky, J., Gazit, E., Rosenman, G.: Ferroelectric and related phenomena in biological and bioinspired nanostructures. Ferroelectrics 399, 107–117 (2010)
[11] Athenstaedt, H.: Permanent Longitudinal Electric Polarisation and Pyroelectric Behaviour of Collagenous Structures and Nervous Tissue in Man and other Vertebrates. Nature 228, 830–834 (1970)
[12] Athenstaedt, H.: Pyroelectric and piezoelectric properties of vertebrates. Ann. NY Acad. Sci. 238, 68–94 (1974)
[13] Lang, S.B.: Pyroelectricity: Occurrence in biological materials and possible physiological implications. Ferroelectrics 34(1), 3–9 (1981)
[14] Athenstaedt, H.: Pyroelectric sensors of organisms. Ferroelectrics 11(1), 365–369 (1976)
[15] Fukada, E.: Piezoelectric properties of biological polymers. Quart. Rev. Biophys. 16(1), 59–87 (1983)
[16] Lang, S.B., Marino, A.A., Berkovic, G., Fowler, M., Abreo, K.D.: Piezoelectricity in the human pineal gland. Bioelectrochem. Bioenerg. 41, 191–195 (1996)
[17] Lang, S.B.: Pyroelectric effect in bone and tendon. Nature 212, 704–705 (1966)
[18] Lang, S.B.: Thermal expansion coefficients and primary and secondary pyroelectric coefficients of animal bone. Nature 224, 798–799 (1969)
[19] Lang, S.B.: Piezoelectricity, pyroelectricity and ferroelectricity in biomaterials - speculation on their biological significance. IEEE Trns. Dielectr. Electr. Insul. 7, 466–473 (2000)
[20] Kryszewski, M.: Fifty years of study of the piezoelectric properties of macromolecular structured biological materials. Acta Phys. Pol. A 105, 389–408 (2004)
[21] Gruverman, A., Rodriguez, B.J., Kalinin, S.V.: Electromechanical Behavior in Biological Systems at the Nanoscale. Springer, New York (2007)
[22] Athenstaedt, H.: Ferroelektrische und piezoelektrische Eigenschaften biologisch bedeutsamer Stoffe. Naturwissenschaften 48(13), 465–472 (1961)
[23] Fröhlich, H.: Long range coherence in biological systems. Riv. del Nuovo Cimento 7, 399 (1977)
[24] von Hippel, A.R.: Proceedings, Second International Meeting on Ferroelectricity. J. Phys. Soc. Japan 28(suppl.), 1 (1970)
[25] Lemanov, V.V., Popov, S.N., Pankova, G.A.: Piezoelectric properties of crystals of some protein aminoacids and their related compounds. Phys. Sol. Stat. 44, 1929–1935 (2002)
[26] Lemanov, V.V., Popov, S.N., Pankova, G.A.: Protein amino acid crystals: Structure, symmetry, physical properties. Ferroelectrics 285, 581–590 (2003)
[27] Hastings, G.W., Elmessiery, M.A., Rakowski, S.: Mechano-electrical properties of bone. Biomaterials 2, 225–233 (1981)
[28] Halperin, C., Mutchnik, S., Agronin, A., Molotskii, M., Urenski, P., Salai, M., Rosenman, G.: Piezoelectric Effect in Human Bones Studied in Nanometer Scale. Nano Lett. 4(7), 1253–1256 (2004)

[29] Minary-Jolandan, M., Yu, M.F.: Nanoscale characterization of isolated individual Type I collagen fibrils: Polarisation and piezoelectricity. Nanotechnology 20, 85706 (2009)
[30] Kholkin, A., Amdursky, N., Bdikin, I., Gazit, E., Rosenman, G.: Strong piezoelectricity in bioinspired peptide nanotubes. ACS Nano 4(2), 610–614 (2010)
[31] Newnham, R.E., Sundar, V., Yimnirun, R., Su, J., Zhang, Q.M.: Electrostriction: Nonlinear Electromechanical Coupling in Solid Dielectrics. J. Phys. Chem. B 101, 10141–10150 (1997)
[32] Kholkin, A.L., Brooks, K.G., Setter, N.: Electromechanical properties of $SrBi_2Ta_2O_9$ thin films. Appl. Phys. Lett. 71(14) (1997)
[33] Beresnev, L.A., Blinov, L.M., Kovshev, E.I.: Dokl. Biophys. 265, 111 (1982)
[34] Beresnev, L.A., Pikin, S.A., Haase, W.: Ferroelectric Polymers. Condensed Matter News 1(8), 13 (1992)
[35] Tasaki, I., Byrne, P.M.: The Origin of Rapid Changes in Birefringence, Light Scattering and Dye Absorbance Associated with Excitation of Nerve Fibers. Japanese J. Physiol. 75 (suppl.), S67–S75 (1993)
[36] Tasaki, I.: Evidence for phase transition in nerve fibres, cells and synapses. Ferroelectrics 220, 305–316 (1999)
[37] Bystrov, V.S.: Ferroelectric Liquid Crystal Models of Ion Channels and Gating Phenomena in Biological Membranes. Ferroelectrics Letters 23, 87–93 (1997)
[38] Shirane, K., Tokimoto, T., Kushibe, H.: Physica D 90, 306 (1996)
[39] Tokimoto, T., Shirane, K., Kushibe, H.: Self-organized chemical model and approaches to membrane excitation. Ferroelectrics 220, 273–290 (1999)
[40] Bystrov, V.S., Lakhno, V.D., Molchanov, A.M.: Ferroelectric-active models of ion channels in biomembranes. J. Theor. Biol. 168, 383–393 (1994)
[41] Gordon, A., Vugmeister, B.E., Rabitz, H., Dorfman, S., Felsteiner, J., Wyder, P.: A ferroelectric model, for the generation and propagation of an action potential and its magnetic field stimulation. Ferroelectrics 220, 291–304 (1999)
[42] Palti, Y., Adelman Jr., W.J.: Measurement of axonal membrane condactances and capacity by means of a varying potential control voltage clamp. J. Memb. Biol. 1, 431–458 (1969)
[43] Leuchtag, H.R.: Fit of the dielectric anomaly of squid axon membrane near heat-block temperature to the ferroelectric Curie-Weiss law. Biophys. Chem. 53, 197–205 (1995)
[44] Ermolina, I., Strinkovski, A., Lewis, A., Feldman, Y.: Observation of Liquid-Crystal-Like Ferroelectric Behavior in a Biological Membrane. J. Phys. Chem. B 105(14), 2673–2676 (2001)
[45] Brown, J.A., Tuszynski, J.A.: A Review of the Ferroelectric Model of Microtubules. Ferroelectrics 220, 141–156 (1999)
[46] Mickey, B., Howard, J.: Rigidity of microtubules is increased by stabilizing agents. J. Cell Biol. 130, 909–917 (1995)
[47] Sataric, M.V., Tuszynski, J.A.: Relationship between the nonlinear ferroelectric and liquid crystal models for microtubules. Phys. Rev. E 67, 11901 (2003)
[48] Tuszynski, J.A., Craddock, T.J.A., Carpenter, E.J.: Bio-Ferroelectricity at the Nanoscale. J. Comp. Theor. Nanoscience 5(10), 2022–2032 (2008)
[49] Tuszynski, J.A., Malinski, W., Carpenter, E.J., Luchko, T., Torin, H.J., Ludena, R.F.: Tubulin electrostatics and isotype specific drug binding. Canadian J. Phys. 86(4), 635–640 (2008)

[50] Hereida, A., Bdikin, I., Kopyl, S., Mishina, E., Semin, S.: Temperature-driven phase Transformation in self-assembled diphenylalanine peptide nanotubes. J. Phys. D: Appl. Phys.: Fast Track Communication 43, 462001 (6 pp) (2010)
[51] Alexe, M., Gruverman, A. (eds.): Nanoscale Characterization of Ferroelectric Materials. Springer, Heidelberg (2004)
[52] Kholkin, A.L., Kalinin, S.V., Roelofs, A., Gruverman, A.: Review of ferroelectric domain imaging by Piezoresponse Force Microscopy. In: Kalinin, S.V., Gruverman, A. (eds.) Scanning Probe Microscopy: Electrical and Electromechanical Phenomena at the Nanoscale, vol. 1, pp. 173–214. Springer, New York (2007)
[53] Schaap, I.A.T., de Pablo, P.J., Schmidt, C.F.: Resolving the molecular structure of microtubules under physiological conditions with scanning force microscopy. Eur. Biophys. J. 33, 462–467 (2004)
[54] Schaap, I.A.T., et al.: Elastic Response, Buckling, and Instability of Microtubules under Radial Indentation. Biophys. 91, 1521–1531 (2006)
[55] Ghiso, J., Plant, G.T., Levy, E., Wisniewski, T., Baumann, M.H.: C-terminal fragments of $\alpha$- and $\beta$-tubulin form amyloid fibrils in vitro and associate with amyloid deposits of familial cerebral amyloid angiopathy. British type. Biochem. Biophys. Res. Commun. 219, 238–242 (1996)
[56] Kalinin, S.V., Rodriguez, B.J., Shin, J., Jesse, S., Grichko, V., Thundat, T., Baddorf, A.P., Gruverman, A.: Bioelectromechanical imaging by scanning probe microscopy: Galvani's experiment at the nanoscale. Ultramicroscopy 106, 334–340 (2006)
[57] Kalinin, S.V., Jesse, S., Rodriguez, B.J., Seal, K., Baddorf, A.P., Zhao, T., Chu, Y.H., Ramesh, R., Eliseev, E.A., Morozovska, A.N., Mirman, B., Karapetian, E.: Recent advances in electromechanical imaging on the nanometer scale: Polarisation dynamics in ferroelectrics, biopolymers, and liquid imaging. Jpn. J. Appl. Phys. 46, 5674–5685 (2007)
[58] Safari, A., Akdogan, K. (eds.): Piezoelectric and Acoustic Materials for Transducer Applications. Springer, New York (2008)
[59] Alexe, M., Hesse, D.: Self-assembled nanoscale ferroelectrics. J. Mater. Sci. 41, 1–11 (2006)
[60] Muralt, P.: Ultrasonic Micromotors Based on PZT Thin Films. J. Electroceram. 3, 143–150 (1999)
[61] Polla, D.L., Erdman, A.G., Robbins, W.P., Markus, D.T., Diaz-Diaz, J., Rizq, R., Nam, Y., Brickner, H.T., Wang, A., Krulevitch, P.: Microdevices in medicine. Ann. Rev. Biomed. Eng. 2, 551–576 (2000)
[62] Hong, E., Krishnaswamy, S.V., Freidhoff, C.B.: Micromachined piezoelectric diaphragms actuated by ring shaped interdigitated transducer electrodes. Sens. Actuat. A 119, 520–526 (2005)
[63] Scott, J.: Ferroelectric Memories. Springer, Berlin (2000)
[64] Ghadiri, M.R., Granja, J.R., Milligan, R.A., McRee, D.E., Hazanovich, N.: Self assembling organic nanotubes based on a cyclic peptide architecture. Nature 366, 324327 (1993)
[65] Aggeli, A., Bell, M., Boden, N., Keen, J.N., Knowles, P.F., McLeish, T.C.B., Pitkeathly, M., Radford, S.E.: Responsive gels formed by the spontaneous self-assembly of peptides into polymeric beta-sheet tapes. Nature 386, 259–262 (1997)
[66] Hartgerink, J.D., Beniash, E., Stupp, S.L.: Self-assembly and mineralization of peptideamphiphile nanofibers. Science 294, 1684–1688 (2001)

[67] Reches, M., Gazit, E.: Casting metal nanowires within discrete self- assembled peptide nanotubes. Science 300, 625–627 (2003)
[68] Zhang, S.: Fabrication of novel biomaterials through molecular self assembly. Nature Biothechnol. 21, 1171–1178 (2003)
[69] Reches, M., Gazit, E.: Controlled patterning of aligned self-assembled peptide nanotubes. Nature Nanotech. 1, 195–200 (2006)
[70] Lovinger, A.J.: Ferroelectric Polymers. Science 220, 1115–1121 (1983)
[71] Naber, R.C.G., Tanase, C., Blom, P.W.M., Gelinck, G.H., Marsman, A.W., Touwslager, F.J., Setayesh, S., Leeuw, D.M.: High-performance solution-processed polymer ferroelectric field-effect transistors. Nature Mater. 4, 243–248 (2005)
[72] Gelinck, G.H., Marsman, A.W., Touwslager, F.J., Setayesh, S., Leeuw, D.M., Naber, R.C.G., Blom, P.W.M.: All-polymer ferroelectric transistors. Appl. Phys. Lett. 87, 092903-3 (2005)
[73] Naber, R.C.G., Boer, B., Blom, P.W.M., Leew, D.M.: Low-voltage polymer field-effect transistors for nonvolatile memories. Appl. Phys. Lett. 87, 203509-3 (2005)
[74] Narayanan, K.N., Bettignies, R., Dabos-Seignon, S., Nunzi, J.M.: A non-volatile memory element based on an organic field-effect transistor. Appl. Phys. Lett. 85, 1823–1825 (2004)
[75] Schroeder, R., Majewski, L.A., Grell, M.: Organic permanent memory transistor using an amorphous, spin-cast ferroelectric-like gate insulator. Adv. Mater. 16, 633–636 (2004)
[76] Hartgerink, J.D., Granja, J.R., Milligan, R.A., Chadiri, M.R.: Self-assembling Peptide nanotubes. J. Amer. Chem. Soc. 118, 43–50 (1996)
[77] Scanlon, S., Aggeli, A.: Self-assembling peptide nanotubes. Nanotoday 3, 22–30 (2008)
[78] Adler-Abramovich, L., Aronov, D., Beker, P., Yevnin, M., Stempler, S., Buzhansky, L., Rosenman, G., Gazit, E.: Self-assembled arrays of peptide nanotubes by vapour deposition. Nature Nanotechnology 4, 849–854 (2009)
[79] Shklovsky, J., Beker, P., Amdursky, N., Gazit, E., Rosenman, G.: Bioinspired peptide nanotubes: Deposition technology and physical properties. Materials Science and Engineering B 169, 62–66 (2010)
[80] Gazit, E.: A possible role for p-stacking in the self-assembly of amyloid fibrils. FASEB J. 16, 77–83 (2002)
[81] Görbitz, C.H.: Nanotube formation by hydrophobic dipeptides. Chem. Eur. J. 7, 5153–5159 (2001)
[82] Görbitz, C.H.: Nanotubes from hydrophobic dipeptides: pore size regulation through side chain substitution. New J. Chem. 27, 1789–1793 (2003)
[83] Görbitz, C.H.: The structure of nanotubes formed by diphenylalanine, the core recognition motif of Alzheimer's b-amyloid polypeptide. Chem. Commun., 2332–2334 (2006)
[84] Sedman, V.L., Adler-Abramovich, L., Allen, S., Gazit, E., Tendler, S.J.B.: Direct observation of the release of phenylalanine from diphenilalanine nanotubes. J. Am. Chem. Soc. 128, 6903–6908 (2006)
[85] Kol, N., Adler-Abramovich, L., Barlam, D., Shneck, R.Z., Gazit, E., Rousso, I.: Self-assembled peptide nanotubes are uniquely rigid bioinspired supramolecular structures. Nano Lett. 5, 1343–1346 (2005)

[86] Harkany, T., Hortobágyi, T., Sasvári, M., Kónya, C., Penke, B., Luiten, P.G.M., Nyakas, C.: Neuroprotective approaches in experimental models of $\beta$-Amyloid neurotoxicity: Relevance to Alzheimer's disease. Prog. Neuropsychopharmacol. Biol. Psychiatry 23, 963 (1999)
[87] HyperChem 7.5, Tools for Molecular Modeling; HyperChem 8.0, Professional Edition. Hypercube. Inc., Gainesville (2002 - 2010)
[88] Landolt, H., Bornstein, R.: Numerical Data and Functional Relationships in Science and Technology (New Series), vol. III/16. Springer, Berlin (1981)
[89] Adler-Abramovich, L., Reches, M., Sedman, V.L., Allen, S., Tendler, S.J.B., Gazit, E.: Thermal and Chemical Stability of Diphenylalanine Peptide Nanotubes: Implications for Nanotechnological Applications. Langmuir 22, 1313 (2006)
[90] de Gennes, P.G., Prost, J.: The Physics of Liquid Crystals. Clarendon, Oxford (1993)
[91] Bernstein, J.: Polymorphism in Molecular Crystals. Clarendon, Oxford (2002)
[92] Scott, J.F., Fan, H.J., Kawasaki, S., Banys, J., Ivanov, M., Macutkevic, J., Blinc, R., Laguta, V.V., Cevc, P., Liu, J.S., Kholkin, A.L.: Terahertz Emission from Tubular $Pb(Zr,Ti)O_3$ Nanostructures. Nano Lett. 8, 4404 (2006)
[93] Nakanishi, T., Okamoto, H., Nagai, Y., Takeda, K.: Synthesis and atomic force microscopy observations of the single-peptide nanotubes and their micro-order assemblies. Phys. Rev. B 66, 165417 (2002)
[94] Yan, X., Zhua, P., Li, J.: Self-assembly and application of diphenylalanine-based nanostructures. Chem. Soc. Rev. 39, 1877–1890 (2010)
[95] Saez, I.M., Goodby, J.W.: Supermolecular liquid crystals. J. Mater. Chem. 15, 26–40 (2005)
[96] Fandrich, M., Meinhardt, J., Grigorieff, N.: Structural polymorphism of Alzheimer A$\beta$ and other amyloid fibrils. Prion 3(2), 89–93 (2009)
[97] Raudenkol, S., Wartewig, S., Neubert, R.H.H.: Polymorphism of ceramide 6: a vibrational spectroscopic and X-ray powder diffraction investigation of the diastereomers of N-($\alpha$-hydroxyoctadecanoyl)-phytosphingosine. Chem. Phys. Lipids 133(1), 89–102 (2005)
[98] Livolant, F., Leforestier, A., Durand, D., Doucet, J.: Structure of dna mesophases. Lect. Notes Phys. 415, 33 (1993)
[99] Abeygunaratne, S., Jakli, A.J., Milkereit, G., Sawade, H., Vill, V.: Antiferroelectric ordering of amphiphilic glycolipids in bent-core liquid crystals. Phys. Rev. E 69, 21703 (2004)